2014

Transient pressure drop correlation between parallel minichannels during flow boiling of R134a

Dolaana M. Khovalyg
University of Illinois at Urbana-Champaign, USA / ITMO University, Russian Federation, khovalyg.d@gmail.com

Predrag S. Hrnjak
University of Illinois at Urbana-Champaign, USA, pega@illinois.edu

Anthony M. Jacobi
University of Illinois at Urbana-Champaign, USA, a-jacobi@illinois.edu

Transient pressure drop correlation between parallel minichannels during flow boiling of R134a

Dolaana M. KHOVALYG[1,2], Pega S. HRNJAK[1], Anthony M. JACOBI[1*]

[1]Department of Mechanical Science and Engineering,
University of Illinois at Urbana-Champaign
Urbana, IL, USA, 61801
Tel: +1(217)333-3115, Fax: +1(217)333-1942, Email: a-jacobi@illinois.edu

[2] Institute of Refrigeration and Biotechnologies
University of Information Technologies, Mechanics and Optics (ITMO University)
Saint-Petersburg, Russian Federation, 191002
Tel: +7(925)851-13-93, Email: khovalyg@illinois.edu

*Corresponding Author

ABSTRACT

There is significant interest in the boiling performance of refrigerants in mini- and microchannels, especially in flow geometries relevant to compact heat exchangers for air-conditioning and refrigeration applications. Pressure drop (ΔP) characteristics during flow boiling of refrigerant R134a have been studied extensively over the past decade; however, in most research ΔP is measured over a single channel or multiple parallel channels (manifold to manifold). There has been no work examining the individual pressure drop in each channel in multiple channel design. Moreover, correlations or relationships between the instantaneous ΔP in individual minichannels operating in parallel have not been reported.

In this work, an investigation of the effect of heat flux, mass flux and inlet vapor qualities on the flow patterns and pressure drop for flow boiling of R134a in 0.54 mm square parallel minichannels is reported. In particular, flow boiling experiments are conducted at flow rates between 0.1 and 0.51 g/s and heat fluxes from 0 to 36 kW/m^2. The heat flux input among a set of four horizontal, parallel minichannels is individually varied and controlled in each test. The focus of the work is on the investigation of correlations between flow boiling of R134a in parallel minichannels based on flow visualization and pressure drop measurements in each channel independently.

1. INTRODUCTION

Hydrodynamic parameters of flow boiling for various refrigerants in mini- and microchannels have been studied extensively over the past decade because of their wide application in microelectronics cooling, air-conditioning and refrigeration. Stable and unstable flow boiling in single and multiple small passages have been examined by Bergles *et al.* (2003), Balasubramanian and Kandlikar (2005), Wang *et al.* (2007), Szczukiewicz *et al.* (2013), Tuo and Hrnjak (2014). An extensive review of two-phase flow instabilities in narrow spaces was reported by Tadrist (2007). However, limited information regarding the inter-channel relationship during flow boiling in mini- and mircochannels subjected to unbalanced heating was found in the literature. Existing studies on the coupling between heat and mass flux in several parallel unevenly heated tubes have been done for tubes with diameter larger than 3 mm. Kakac *et al.* (1977), Lee and Pan (1999), Baikin *et al.* (2011) investigated stability of in-tube boiling and flow distribution in unevenly heated system from 2 to 6 parallel channels. Kakac *et al.* (1977) studied the phenomena in each channel by means of pressure and temperature measurements. Flow rate was examined in every single tube by Lee and Pan (1999) and Baikin *et al.* (2011). It was determined that the most heated tube exhibits the largest magnitude of oscillations, and more mass of working fluid flow through less heated pipe. The technical challenges to measure pressure drop and flow rate in each tiny channel might be the major reason of the absence of similar research in smaller scales, although such study can present an added value to the actual knowledge in the area of flow boiling mechanisms in narrow channels.

The focus of this work is on the investigation of interaction between the flow in neighboring 0.54 mm hydraulic diameter minichannels subjected to different operating conditions, such as varying mass and heat flux. The refrigerant R134a was selected as it is one of the most widely used working fluids in air-conditioning and refrigeration systems. ΔP signals were recorded with high frequency in order to capture transient changes of the variables. The existence and the strength of the inter-channel relationship was estimated by correlation analysis of transient pressure drop signal (ΔP) across each channel.

2. EXPERIMENTAL METHOD

2.1. Experimental Apparatus and Test section

Fig.1 illustrates the experimental setup and the test section is shown in Fig. 2.

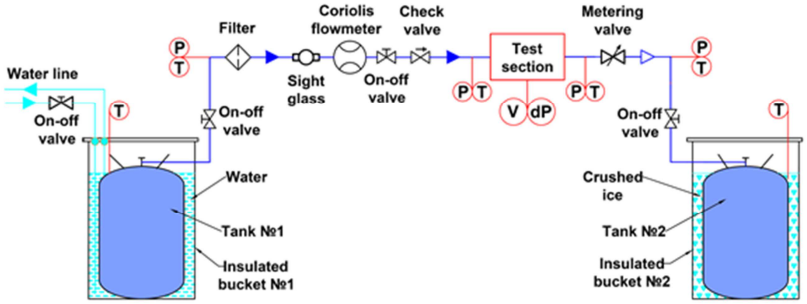

Figure 1: Experimental setup

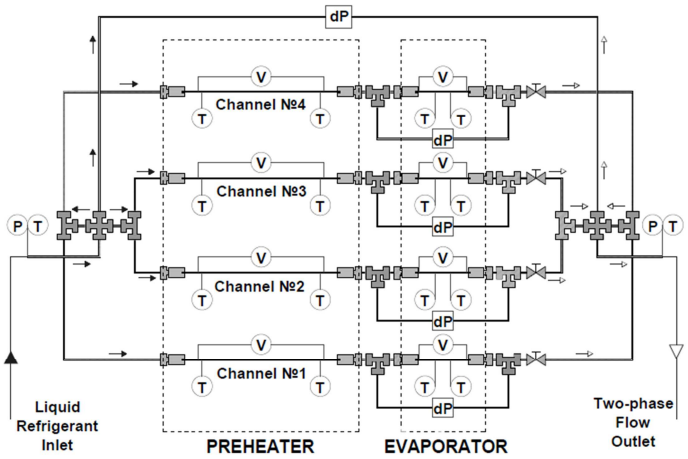

Figure 2: Test section

The refrigerant R134a flow through the test section was driven by the pressure difference between the beginning and the end of the experimental loop; no pump was used in the experiment. Total flow rate was measured using a Coriolis-type flowmeter installed upstream of the test section. A metering valve right after the test section was used to adjust the flow rate of the refrigerant. The refrigerant distribution within the test section was arranged using brass fittings: a cross-fitting divided the incoming flow from the main feeding tube of 1.65 mm (ID) into two equal parts and further downstream two T-type fittings split each portion into two flows.

The test section consisted of a preheater and an evaporator. Four stainless steel tubes with circular cross-section of 0.508 mm and 200.2 mm in length were used for preheating the refrigerant by means of direct Joule heating. The vapor quality was varied in the preheating section that partially evaporated the refrigerant before it entered the evaporator. Four square glass channels from quartz with inner cross-section of 0.538x0.538 mm^2 and 76.8 mm in length were used in the evaporative section. A thin film of Tungsten was sputtered on an outer wall of each glass tube in order to apply direct current; flow visualization using high-speed video camera was made available through three transparent walls. Each preheating stainless steel tube and each glass tube had its own DC

power supply in order to individually control the applied heat flux. Shut-off valves were mounted at the end of each of four minichannels in order to be able to regulate the number of channels involved in the experiment each time.

Pressure transducers and immersed shielded thermocouples installed at the beginning and at the end of the test section were used to measure inlet and outlet parameters of the refrigerant. Four differential pressure transducers of «wet-wet» type were measuring the pressure difference (ΔP) across each glass minichannel. Pressure losses due to the intermediate connectors were negligible; therefore, the signal from the pressure transducers was considered as the original value of ΔP across the relevant minichannel. Uncertainties of parameters involved in the experiments are given in Table 1.

Table 1: Uncertainties in measurements

Parameter	ṁ	P	ΔP_1	ΔP_2	ΔP_3	ΔP_4	T	q_{preh}	q_{evap}	x
Units	g/s	kPa	kPa	kPa	kPa	kPa	°C	%	%	--
Value	0.01	4.6	*0.033*	*0.010*	*0.035*	0.043	0.2	5	5	0.01

2.2. Data reduction

Once the system reached steady state conditions, each parameter (pressure, temperature and flow rate) was recorded at frequency 2000 Hz over 120 seconds. The measured data were filtered from high frequency noise and processed in MATLAB®; the extended statistical analysis was undertaken afterwards.

It is well known that pressure drop in mini- and microchannels highly depends on flow patterns; it is a strong function of flow rate, heat flux and vapor quality (Grzybowski and Mosdorf (2014), Tuo and Hrnjak (2014)). Therefore, the mean ΔP and the fluctuations were compared seeking insight about flow phenomena in each channel. Variation in average ΔP also was interpreted as an indicative parameter of flow distribution between channels. Power spectral analysis of pressure drop signals provides valuable information about the dominant frequency associated with the studied phenomena. A power spectral density (PSD) curve illustrates the decomposition of a process into different frequencies that are present in a signal and helps to identify periodicities. The frequency corresponding to maximum PSD value indicates the most influential periodical event occuringe during flow boiling. Comparisons of peak frequencies for each pressure drop signal were undertaken for each test in order to analyze the different events occurring in channels under changing heat and mass flux conditions.

The cross-correlation coefficient is a widely used measure of strength and direction of relationships between two sets of variables. It can be applied to different types of signals as long as they have the same number of variables. Transient pressure drop signals in each minichannel and pressure signals in inlet and outlet manifolds were used to compute the dimensionless time-lagged linear cross-correlation coefficient $\boldsymbol{r}$. According to Bendat and Piersol (2010), the mathematical formula for normalized time-lagged linear $\boldsymbol{r}$ for two random X and Y data series consisting of N values is:

$$r = \frac{1}{N}\frac{\sum(X_i - \overline{X_N})(Y_{i-1} - \overline{Y_{N-1}})}{\sigma_{X_i}\sigma_{Y_{i-1}}} \quad (1)$$

The average cross-correlation coefficient was determined over 120 seconds long set of data, and the maximum ($\boldsymbol{r}_{max}$) and minimum ($\boldsymbol{r}_{min}$) values of the average coefficient were determined. The maximum values between $|\boldsymbol{r}_{max}|$ and $|\boldsymbol{r}_{min}|$ indicate the strength of the linear correlation between two comparing variables; the sign of the maximum coefficient indicates the direction of the relationship between signals. The interpretation of the correlation power can vary, depending on the examined phenomena. The coefficient of determination ($\boldsymbol{r}^2$) was further calculated in order to quantify the percentage of the correlated data.

3. RESULTS AND DISCUSSIONS

Study of the existence of the correlation between channels was undertaken by conducting several conditions:

Type I tests: one channel is diabatic, and the other channels are adiabatic (single phase liquid flow).

Type II tests: equal heat fluxes are applied to all four channels.

Type III tests: different constant heat fluxes are applied to three preheating channels, the heat flux of the fourth channel is varied.

3.1. Type I tests

The heat is applied to only one channel during these tests; single phase liquid refrigerant is flowing through the other channels. During the tests, glass channel №1 has an imposed heat flux of 36.5 kW/m^2, the saturation

temperature is T=29.1°C, and the total flow rate is varied (see Table 2). Bubble formation is observed at the beginning of the glass tube in each test and exit vapor quality depends on the flow rate. Estimated average x_{evap_exit} is listed in Table 2. At the highest flow rate ṁ = 0.51 g/s short slugs were observed at the glass tube outlet; slugs elongate as the flow rate decreases, and long slugs were observed at the glass tube outlet at the lowers flow rate ṁ = 0.20 g/s.

Table 2: Type I test conditions

Parameters	Unit	Value
q_{evap1}	kW/m^2	36.5
ṁ	g/s	0.20, 0.29, 0.41, 0.51
x_{evap_exit}	--	0.157, 0.107, 0.076, 0.061

The mean pressure drop and the fluctuations in each channel for Type I tests are illustrated in Fig. 3. The bar lines below and above average values depict minimum and maximum of signals. It is clear that pressure drop fluctuations of a heated channel with flow boiling are more significant than in adiabatic channels filled with only liquid phase refrigerant. Pressure drop and flow rate of two-phase flow in minichannels significantly oscillates because bubbles grow rapidly in small passages. Periodic pressure drop oscillation and flow patterns alternation during flow boiling were observed due to dynamic flow rate changes.

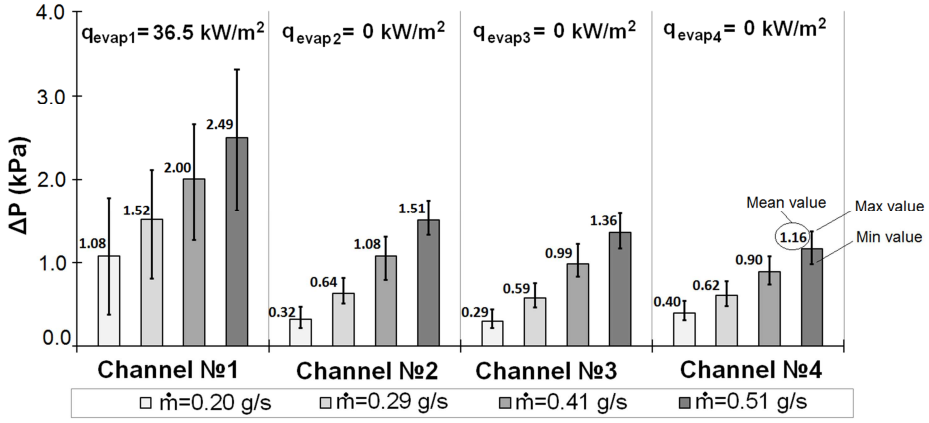

Figure 3: Mean values and amplitude of ΔP_1, ΔP_2, ΔP_3, ΔP_4 (Test conditions Type I)

Power spectral density functions for Type I tests are illustrated in Fig. 4. The plots show the power carried by ΔP signals per unit frequency. It is apparent that the diabatic channel №1 always shows the greatest power magnitude in comparison to the other three adiabatic channels. Moreover, the peak frequencies of adiabatic channels depend on the peak frequency of the heated channel as flow oscillations in channel №1 cause similar flow fluctuations in other liquid-phase filled channels. The frequencies that correspond to the maximum PSD shift to higher magnitude when flow rate increases and it is associated with periodic bubbly flow oscillations. When flow rate augments the boiling process becomes more stable.

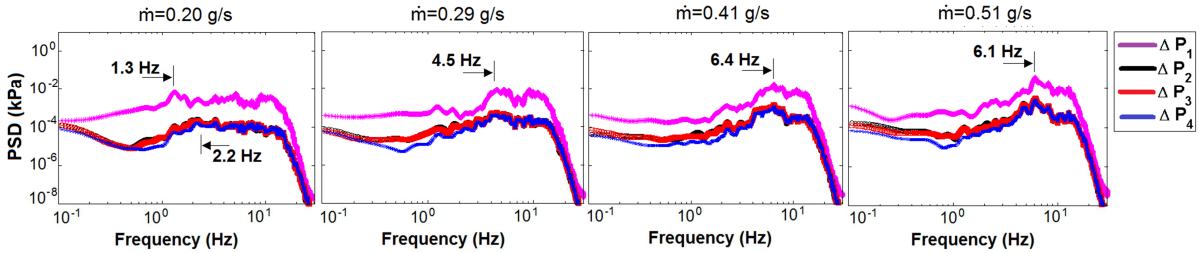

Figure 4: Power ΔP_1, ΔP_2, ΔP_3, ΔP_4 and (b) P_{in}, P_{out} (q_{evap1} = 36.5 kW/m^2, $q_{evap\ 2,3,4}$ = 0 kW/m^2, ṁ = 0.51 g/s)

Cross-correlation analysis results are shown in Table 3. They reveal that pressure drop signals in adiabatic channels have negative relationship with the heated channel for total flow rates more than ṁ=0.2 g/s. ΔP signals in channels with single phase are out of phase with ΔP_1 signal in the diabatic channel №1. Coefficient ***r*** of adiabatic channels increases as the mass flux increases and the vapor quality in diabatic channel decreases. Scatter plots of the

normalized cross-correlation curves illustrate periodicity of pressure drop signals and the relationship between them. Fig. 5 depicts the normalized cross-correlation curves for pressure drop signals at total flow rate ṁ=0.51 g/s. Fig.5a shows that ΔP_2, ΔP_3, ΔP_4 are out of phase compared to ΔP_1, and ΔP_1 is out of phase in all other cases (Fig.5b-d). Correlation curves for ΔP_2, ΔP_3, ΔP_4 fall almost on top of each other, and it proves that flow behavior in the three adiabatic channels is almost identical.

Table 3: Type I tests cross-correlation coefficients **r** and coefficients of determination $\mathbf{r^2}$ in italics.

	ΔP 1	ΔP 2	ΔP 3	ΔP 4	ΔP 1	ΔP 2	ΔP 3	ΔP 4	ΔP 1	ΔP 2	ΔP 3	ΔP 4	ΔP 1	ΔP 2	ΔP 3	ΔP 4
	ṁ = 0.20 g/s				ṁ = 0.29 g/s				ṁ = 0.41 g/s				ṁ = 0.51 g/s			
ΔP 1		*0.409*	*0.398*	*0.400*		*0.566*	*0.583*	*0.653*		*0.724*	*0.736*	*0.811*		*0.775*	*0.803*	*0.859*
ΔP 2	0.640		*0.917*	*0.858*	-0.753		*0.956*	*0.918*	-0.851		*0.955*	*0.931*	-0.880		*0.967*	*0.949*
ΔP 3	0.631	0.957		*0.892*	-0.764	0.978		*0.933*	-0.858	0.977		*0.942*	-0.896	0.983		*0.940*
ΔP 4	0.632	0.944	0.926		-0.808	0.966	0.958		-0.901	0.970	0.965		-0.927	0.970	0.974	

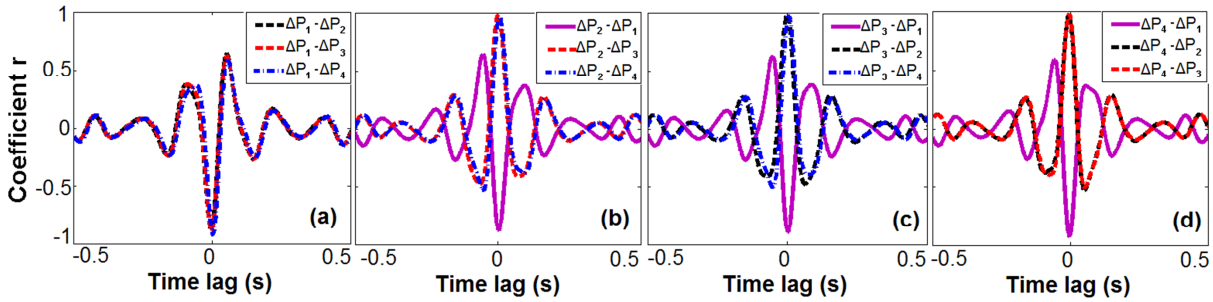

Figure 5: Normalized cross-correlation curves of (a) ΔP_1, (b) ΔP_2, (c) ΔP_3, (d) ΔP_4 (ṁ = 0.51 g/s, Type I test).

The cross-correlation coefficient of heated channel №1 grows from 0.63 up to 0.93 when flow rate increases. It can be concluded that dynamic pressure drop signals are similar to each other when less vapor is generated in channels and less flow perturbation takes place. Generation of vapor in channel №1 causes flow rate oscillation in the entire test section; thus, flow in other adiabatic channels fluctuates in a similar manner.

3.2. Type II tests

An equal heat flux of q_{preh}=2.15 kW/m^2 is applied to all four stainless steel tubes in the preheating section and the glass channels in the evaporating section remain adiabatic. The saturation temperature of R134a is T = 25.5^{o}C and the total flow rate is varied (see Table 4). The estimated average vapor qualities at the outlet of each preheating tube x_{preh_exit} listed in Table 4 show that as flow rate increases vapor quality lessens. Bubbly-slug flow steadily flowing forward was observed in all four glass channels at 4 different flow rates

Table 4: Type II test conditions

Parameters	Unit	Value
q_{preh}	kW/m^2	2.15
q_{evap}	kW/m^2	0
ṁ	g/s	0.19, 0.30, 0.39, 0.50
x_{preh_exit}	--	0.092, 0.084, 0.079, 0.076

Average pressure drop values during Type II tests and their fluctuations are depicted in Fig. 6. It is expected that when individually controlled equal heat flux is applied to each preheating tube then even flow distribution and nearly equal pressure drops in each channel would be observed. However, the measured pressure drop values show that maldistribution among the channels occurs. The ratio of ΔP_i to the lowest ΔP is given in Table 5. This ratio can be used to estimate the differences in flow distribution between channels.

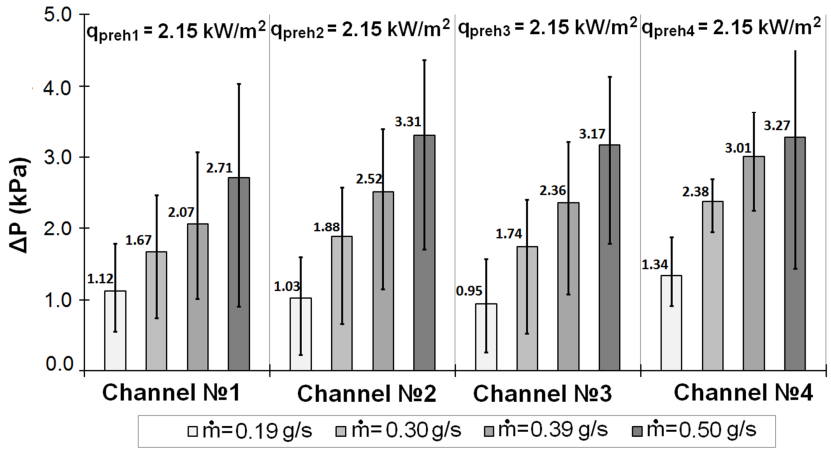

Figure 6: Mean, minimum and maximum values of $\Delta P_1, \Delta P_2, \Delta P_3, \Delta P_4$ (Test conditions Type II).

Table 5: Ratio of pressure drop differences distribution between channels (Type II tests)

Flow rate (g/s)	Channel №1	Channel №2	Channel №3	Channel №4
0.19	1.00	1.22	1.17	1.21
0.30	1.00	1.22	1.14	1.45
0.39	1.00	1.13	1.04	1.43
0.50	1.18	1.08	1.00	1.41

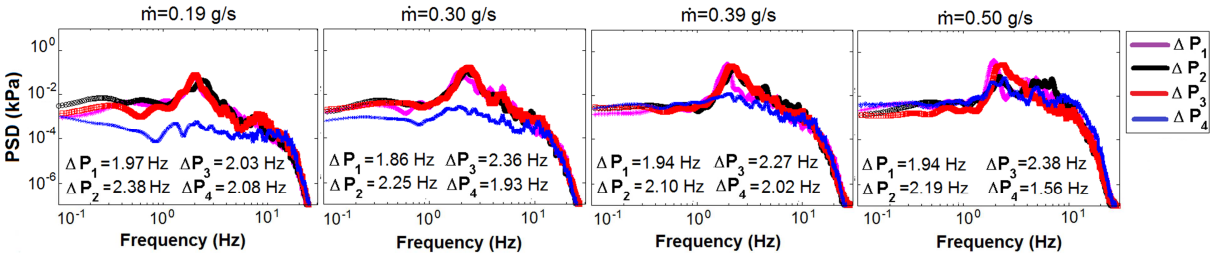

Figure 7: Power spectral density (PSD) functions of $\Delta P_1, \Delta P_2, \Delta P_3, \Delta P_4$ (Type II tests).

Cross-correlation analysis results for Type II tests are shown in Table 6. The cross-correlation between channels is less than 0.15, and the coefficient of determination does not exceed 0.02. It can be seen, that channel №4 is in phase with all the other channels when total flow rate is below ṁ=0.50 g/s. Channel №1 is out of phase with channel №2 and vice-versa. Normalized cross-correlation curves for every pressure drop signal at flow rate ṁ=0.50 g/s are given in Fig. 8 as an illustration of correlation behavior for Type II tests. It is clear that the correlation curves are less harmonic and do not resemble each other in comparison with Type I tests. The overall analysis of coefficients of determination $\mathbf{r}^2$ shows that no more than 2% of ΔP_i variables correlate with each other when equal heat flux applied and similar flow patterns observed in each channel.

Table 6: Type II tests cross-correlation coefficients **r** and coefficients of determination $\mathbf{r}^2$ in italics.

	ΔP 1	**ΔP 2**	**ΔP 3**	**ΔP 4**	**ΔP 1**	**ΔP 2**	**ΔP 3**	**ΔP 4**	**ΔP 1**	**ΔP 2**	**ΔP 3**	**ΔP 4**	**ΔP 1**	**ΔP 2**	**ΔP 3**	**ΔP 4**
	ṁ = 0.19 g/s				**ṁ = 0.30 g/s**				**ṁ = 0.39 g/s**				**ṁ = 0.50 g/s**			
ΔP 1		*0.011*	*0.012*	*0.015*		*0.008*	*0.008*	*0.019*		*0.010*	*0.007*	*0.006*		*0.008*	*0.005*	*0.011*
ΔP 2	-0.106		*0.011*	*0.011*	-0.091		*0.012*	*0.026*	-0.099		*0.009*	*0.003*	-0.092		*0.006*	*0.003*
ΔP 3	-0.108	-0.104		*0.015*	-0.091	0.111		*0.016*	0.081	0.096		*0.005*	-0.068	0.074		*0.007*
ΔP 4	0.124	0.103	0.121		0.137	0.160	0.128		0.075	0.057	0.071		0.103	-0.059	-0.083	

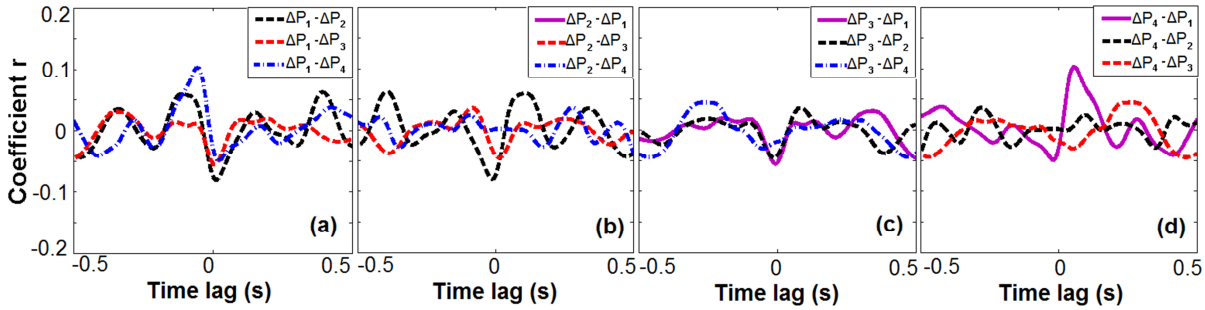

Figure 8: Normalized cross-correlation curves of (a) ΔP_1, (b) ΔP_2, (c) ΔP_3, (d) ΔP_4 ($\dot{m}$ = 0.50 g/s, Type II test).

3.4. Type III tests

Type III tests are conducted to study the effect flow boiling phenomena in one channel potentially have on the other three diabatic channels by varying the applied heat flux and keeping heat fluxes on other channels constant (Table 6). Moreover, the heat flux on channel №1 is matched to the heat flux applied on the neighboring channel in order to examine possible coupling effects of two channels. Each glass channels is kept at the same heat fluxes q_{evap}= 2.2 kW/m^2. Saturation temperature is T=29.3 ^{o}C.

Table 6: Type III test conditions

Test №	Parameter	Unit	Channel №			
			№ 1	№ 2	№ 3	№ 4
1	q_{preh}	kW/m^2	9.64	4.50	5.80	6.80
2			**7.12**	4.50	5.80	**6.80**
3			**5.96**	4.50	**5.80**	6.80
4			**4.75**	**4.50**	5.80	6.80
5			2.86	4.50	5.80	6.80
	q_{evap}	kW/m^2	2.2			
	$\dot{m}$	g/s	0.1, 0.34			

Experiments were conducted for two different flow rates of $\dot{m}$=0.1 g/s and $\dot{m}$=0.34 g/s. The different flow patterns observed in glass channel № 1 during tests using high-speed video recording as well as estimated average vapor qualities *x* are illustrated in Fig. 9. It is apparent, that vapor quality at lower flow rate 0.1 g/s was always higher. Moreover, dry out was noted when the highest heat flux at q_{preh1}=9.64 kW/m^2 was applied to the channel.

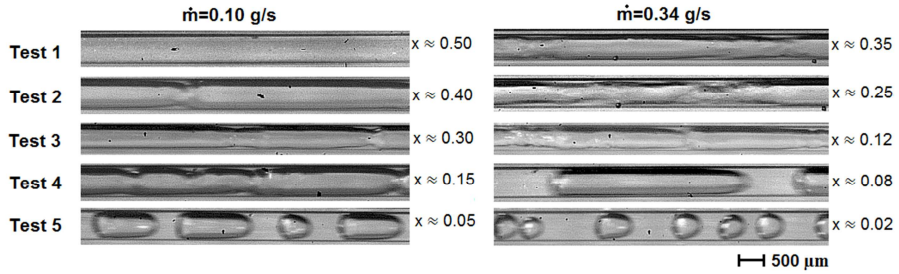

Figure 9: Typical flow patterns observed in channel №1 during Type III tests.

The mean pressure drop values and the fluctuations for Type III tests are shown in Fig. 10. It is noticeable that when the applied heat flux increases, ΔP_1 decreases when the flow rate is $\dot{m}$=0.10 g/s. The opposite result occurs in the case of $\dot{m}$=0.34 g/s. At lower flow rates more vapor generation leads to flow pattern transition from slug flow to complete dry out. As a result, the thin film around tube walls completely evaporates and the measured pressure drop corresponds to the vapor phase. The opposite situation is observed when flow rate increases, two-phase flow is observed inside a minichannel in all range of examined heat fluxes. The bar chart in Fig. 10 also shows that pressure drop in channels №2, 3, and 4 subjected to constant heat fluxes increase as the heat flux applied to channel №1 rises for both flow rates. It occurs as the heat flux applied to the channel №1 increases and higher vapor generation rate

leads to less inlet of liquid flow into the channel. Since the flow rate entering into the test section is constant, flow rates through the other three channels escalate when flow rate through one channel decreases.

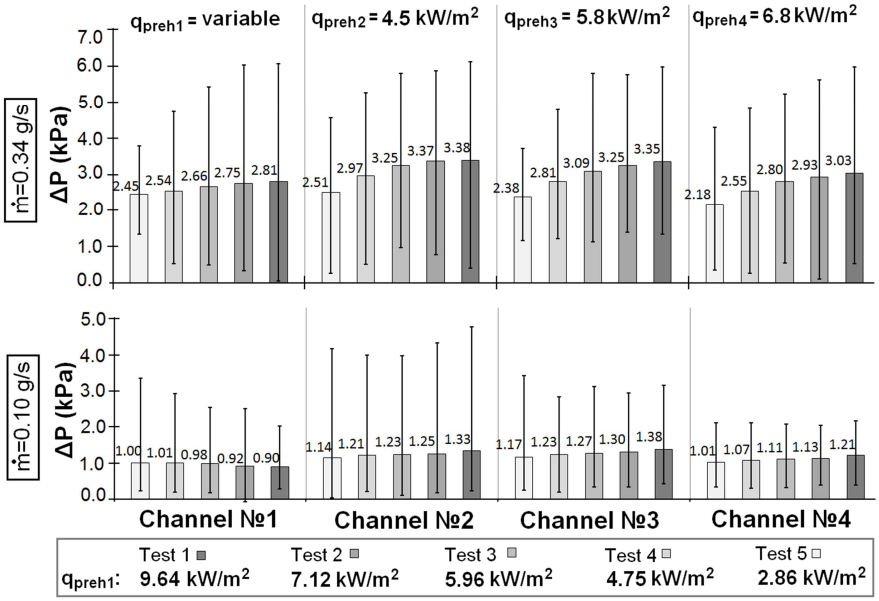

Figure 10: Mean, minimum and maximum values of $\Delta P_1, \Delta P_2, \Delta P_3, \Delta P_4$ (Test conditions Type III).

Power spectral density curves for Type III tests are shown in Fig. 11. Peak frequencies of ΔP signal in channels 2, 3, and 4 stay almost the same from the various tests; additionally, a dominant frequency augments as the applied heat flux and flow rate increase. First and foremost, this phenomenon is linked to vapor quality and the associated flow patterns in each channel. At high flow rates and low heat fluxes small bubbles and short slugs demonstrate high frequencies in the power density spectrum. On the other hand, when the flow rate decreases and the applied heat flux rises, semi-annular and annular flow is observed and changes in flow structures occur over time intervals. As applied heat flux increases the peak frequency in PSD spectrum for channel №1 increase at constant fow rate ṁ =0.1 g/s. However, a similar trend is not observed at higher flow rate ṁ = 0.34 g/s. PSD curves illustrate that there are several major frequency modes present. The two columns with frequencies under the PSD curves of ΔP_1 at 0.34 g/s in Fig. 11 refer to the first and the second peak in power density spectrum. By examining closer the flow patterns one can conclude that the different frequency modes correspond to the alternation of long and short slugs in channel №1.

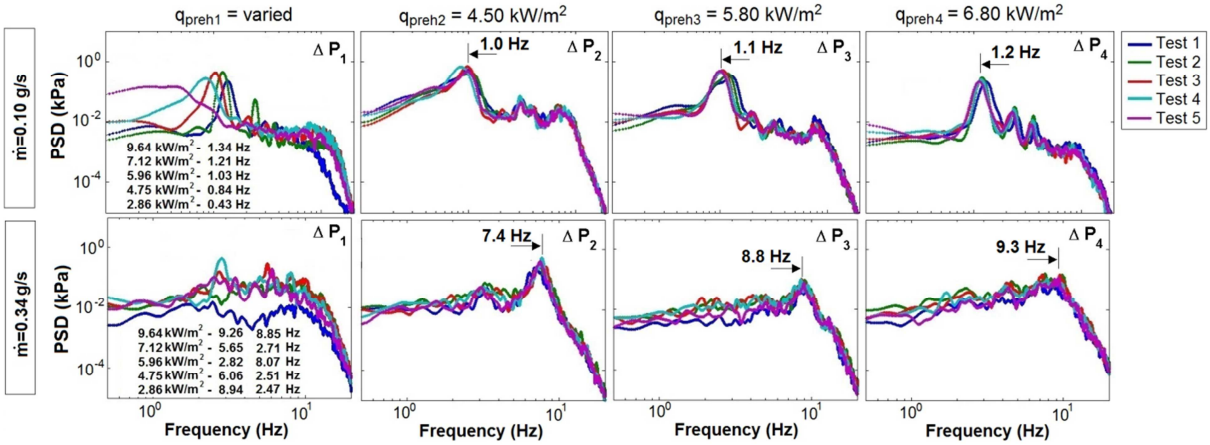

Figure 11: Power spectral density (PSD) functions of $\Delta P_1, \Delta P_2, \Delta P_3, \Delta P_4$ (Type III tests).

Cross-correlation coefficients ***r*** and coefficients of determination r^2 for Type III tests are presented in Table 7. It can be concluded from the table, that ΔP_1 signals for tests conducted at 0.10 g/s correlate the most with a

channel subjected to nearly equal heat flux with channel № 1 such as channel №4 in Test 2, channel №3 in Test 3 and channel №2 in Test 4. It is also clear that as heat flux applied to channel №1 decreases, the correlation magnitude between ΔP_1 and ΔP_4 decreases as it is shown in Fig. 11. These observations indicate that the channels correlate well with each other when similar flow patterns are observed and the behavior of pressure drop signals is analogous. However, for tests conducted at flow rate $\dot{m}$=0.34 g/s the same trend is observed only during Test 5, when the applied heat fluxes were set in an increasing order from channel №1 to №4. ΔP_2 and ΔP_3 signals correlate the most for all the other tests at $\dot{m}$=0.34 g/s, showing that those two channels have similar flow modes. Comparison of coefficients of determination $\mathbf{r}^2$ shows that up to 30% of ΔP_i variables correlate with each other at $\dot{m}$=0.10 g/s, while no more than 2.7% of variables correlate at flow rate 0.34 g/s.

The normalized cross-correlation curves for Type III tests pressure drop signal at flow rate ṁ=0.34 g/s are given in Fig. 12. In comparison with Type II tests the correlation curves are more periodic and have distinct patterns. Type II tests were conducted at heat flux 2.15 kW/m^2 and extremely low vapor qualities were observed. For Type III tests heat flux was greater than 2.86 kW/m^2 and vapor qualities were higher. Therefore, the differences in normalized cross-correlation curves show that at higher heat fluxes the pressure drop signals are more dynamic and variable.

Table 7: Type III tests cross-correlation coefficients **r** and coefficients of determination $\mathbf{r}^2$ in italics.

		ΔP 1	ΔP 2	ΔP 3	ΔP 4	ΔP 1	ΔP 2	ΔP 3	ΔP 4	ΔP 1	ΔP 2	ΔP 3	ΔP 4	ΔP 1	ΔP 2	ΔP 3	ΔP 4	ΔP 1	ΔP 2	ΔP 3	ΔP 4
		Test 1				Test 2				Test 3				Test 4				Test 5			
0.10 g/s	ΔP 1		*0.055*	*0.141*	*0.306*		*0.037*	*0.156*	*0.227*		*0.049*	*0.084*	*0.027*		*0.053*	*0.034*	*0.011*		*0.032*	*0.009*	*0.007*
	ΔP 2	0.234		*0.036*	*0.038*	0.191		*0.055*	*0.029*	0.222		*0.053*	*0.030*	0.230		*0.052*	*0.019*	-0.179		*0.144*	*0.036*
	ΔP 3	0.375	0.190		*0.137*	0.394	0.234		*0.166*	0.291	-0.230		*0.030*	0.184	-0.229		*0.053*	0.093	0.380		*0.072*
	ΔP 4	0.553	0.194	0.371		0.476	0.169	-0.407		0.165	0.174	0.174		0.105	0.138	0.231		0.084	0.190	0.268	
0.34 g/s	ΔP 1		*0.005*	*0.006*	*0.003*		*0.004*	*0.003*	*0.004*		*0.005*	*0.004*	*0.006*		*0.004*	*0.005*	*0.004*		*0.022*	*0.015*	*0.003*
	ΔP 2	0.072		*0.026*	*0.008*	-0.059		*0.019*	*0.003*	0.069		*0.020*	*0.007*	0.066		*0.027*	*0.017*	0.147		*0.010*	*0.005*
	ΔP 3	0.080	0.162		*0.004*	0.052	0.138		*0.007*	0.065	0.141		*0.016*	0.073	0.163		*0.012*	0.124	0.100		*0.005*
	ΔP 4	-0.055	0.088	0.065		0.062	-0.058	0.085		0.077	0.082	0.126		0.066	0.129	0.111		-0.051	-0.069	-0.072	

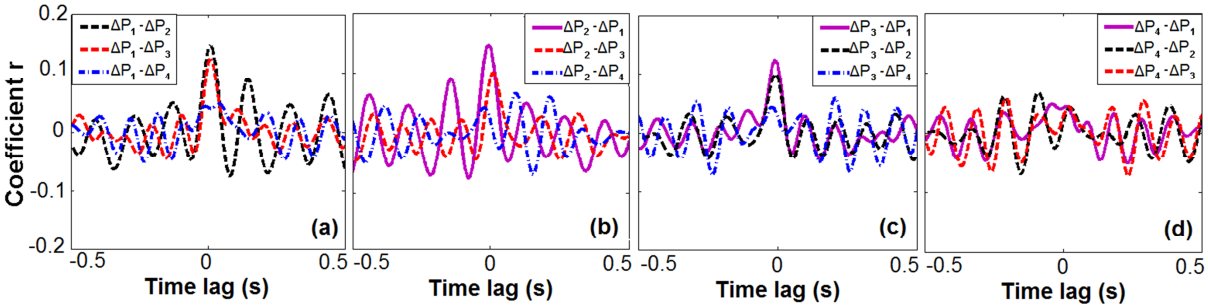

Figure 12: Normalized cross-correlation curves of (a) ΔP_1, (b) ΔP_2, (c) ΔP_3, (d) ΔP_4 (ṁ = 0.34 g/s, Test 5).

4. CONCLUSIONS

Analysis of the transient pressure drop measurements during flow boiling of R134a in parallel square minichannels having a hydraulic diameter of 0.54 mm is reported in this work. The research is aimed at the study of the interactions between channels, and to determine the strength of the relationships when different flow patterns are observed in neighboring minichannels. The design of the experimental test section enabled measurement of pressure drop in each channel and to vary independently the applied heat flux in preheating and evaporating sections. Three different types of experiments were conducted at various flow rates. Type I tests were focused on the comparison of the flow behavior in a single diabatic channel. Study of the correlation between equally heated four parallel channels was undertaken with Type II tests. Type III tests were conducted to investigate the potential coupling effect when heat flux applied to a single channel is varied while the other three channels are subjected to constant heat fluxes.

From the analysis of transient pressure drop oscillation, and comparisons of PSD curves and cross-correlation coefficients, one can conclude the following: First of all, flow maldistribution takes place even when equal low heat flux is applied to geometrically identical channels. Possible slight difference in roughness, slight deviations of the applied electrical power might be the reason of this phenomenon. Secondly, the boiling process is

more stable when there is less flow perturbation within a channel. Stable boiling is observed when vapor generation does not disturb the upcoming flow. Rapid growth of bubbles occurring in a minichannel either at low flow rates or high heat fluxes causes flow rate oscillation in the channel itself and in all the neighboring channels. Thus, mass flux plays a crucial role in flow boiling stabilization. Thirdly, experimental results of unequally heated minichannels illustrate that establishing the relationship between channels is a complicated task. The correlation parameters such as coefficient **r** and coefficient of determination $\mathbf{r^2}$ in some cases are extremely low, no correlation between channels can be considered. It is noticeable that the **r** and $\mathbf{r^2}$ coefficients decrease when stable flow boiling is observed. Once the rapid growth of bubbles occurs in one or several minichannels then the flow oscillations propagate to all other channels and interaction between channels take place.

NOMENCLATURE

r	cross-correlation coefficient
r^2	coefficient of determination
N	number of data points
X	reference data sequence
Y	correlating data sequence
T	temperature (^oC)
ΔP	pressure drop (kPa)
P	pressure (kPa)
$\dot{m}$	flow rate (g/s)
x	vapor quality
σ	standard deviation

Subscripts:

1	minichannel №1
2	minichannel №2
3	minichannel №3
4	minichannel №4
preh	preheater
evap	evaporator
in	inlet
out	outlet
total	overall value
exit	outlet of a specified channel

REFERENCES

Baikin, M., Taitel Y., Barnea D., 2011, Flow distribution in parallel heated pipes, *International Journal of Heat and Mass Transfer*, 192, pp. 31-49.

Balasubramanian, P., Kandlikar, S. G., 2005, An experimental study of flow patterns and flow instabilities in parallel rectangular minichannels, *Heat Transfer Engineering*, 26, 3: p. 20-27.

Bendat, S. J., Piersol, G.A., 2010, *Random data: analysis and measurement procedures*, J. Wiley & Sons, Hoboken, N.J., p. 640.

Bergles, A.E., Lienhard, J.H., Kendall, G.E., Griffith, P., 2003, Boiling and evaporation in small diameter channels, *Heat Transfer Engineering*, vol. 24, 1: p. 18-40.

Grzybowski H., Mosdorf R., 2014, Dynamics of pressure oscillations in flow boiling and condensation in minichannels, *International Journal of Heat and Mass Transfer*, 73: p. 500-510.

Kakac S., Veziroglu T., N. Ozhoya N., Lee S., 1977, Transient boiling flow instabilities in a multi-channel upflow system, *Wårme Steffubertr*. 10: p. 175–188.

Lee, J. D., Pan C., 1999, Dynamics of multiple parallel boiling channel system with forced flows, *Nuclear Engineering and Design*, 192: p. 31-49.

Szczukiewicz, S., Borhani, N., Thome, J.R., Thome, J. R., 2013, *Two-phase flow operational maps for multi-microchannel evaporators, International Journal of Heat and Fluid Flow*, 42: p. 176-189.

Tadrist, L., 2007, Review on two-phase instabilities in narrow spaces, *International Journal of Heat and Fluid Flow*, 28: p. 54-62.

Tuo, H., Hrnjak, S. P., 2014, Visualization and measurement of periodic reverse flow and boiling fluctuations in a microchannel evaporator of an air-conditioning system, I*nternational Journal of Heat and Mass Transfer*, 71: p. 639-652.

Wang, G., Cheng, P., Wu, H., 2007, Unstable and stable flow boiling in parallel microchannels and in a single microchannel, *International Journal of Heat and Mass Transfer*, 50: p.4297-4310.

ACKNOWLEDGEMENT

This work was financially supported by Air-Conditioning and Refrigeration Center, UIUC.